



Published in final edited form as:

Circ Res. 1966 August ; 19(2): 332–346.

Plasma Indicator Dispersion in Arteries of the Human Leg

James B. Bassingthwaighe, M.D., Ph.D.

From the Section of Physiology, Mayo Clinic and Mayo Foundation, Rochester, Minnesota.

Abstract

Indicator-dilution curves were recorded from the femoral and dorsalis pedis arteries of five normal men after injections of indocyanine green into the superior vena cava or thoracic aorta. By considering the femoral curves as inputs to a mathematically linear system and the dorsalis pedis curves as outputs, transfer functions (the distribution of transit times) for the arterial segment between these sites were obtained in terms of a four-parameter model, the lagged normal density curve, over a sixfold range of flow rates. The parameters of the spread (dispersion) of 57 transfer functions were proportional to the mean transit time. The mean difference between transit time and appearance time was $0.30 \bar{t}$; the square root of the variances was $0.18 \bar{t}$. These linear relationships suggest that flow rate has no significant influence on dispersion and that, since no transition from laminar to turbulent flow was apparent, arterial flow characteristics were not significantly changed over a wide range of flow rates. The secondary implication is that the rate of spatial longitudinal spreading of indicator with distance traveled is primarily a function of the geometry of the arterial system, not of the rate of flow, and, therefore, that the spatial distribution at any instant is a function of this rate and of the distance traveled through the system.

Keywords

arterial blood flow; cardiac output velocity profile; vasodilatation by adenosine triphosphate infusion circulation model; arterial transfer functions distribution of transit times through an arterial segment; indocyanine green indicator dilution; unanesthetized man

Recorded concentration-time curves show the effects of dispersion of indicator at the injection site and in the sampling system. The latter effect can be lessened by the use of sampling systems of high dynamic response, but the former effect is unavoidable. However, circulatory transport through a given segment of the circulation can be characterized experimentally. After injection of indicator at a point upstream from the segment, simultaneous indicator concentration-time curves may be recorded, with identical sampling-recording systems, from the entrance and from the exit of the segment. From these curves, the transfer function of the segment (the frequency distribution of transit times through it) can be estimated.

In this study, the transfer functions were defined in terms of a model—the lagged normal density curve.¹ The flow of blood through the leg was increased by the infusion, at varied constant rates, of adenosine triphosphate in order to assess the influence of flow rate on these transfer functions.

Methods and Computations

Five normal men were studied while they were awake in the supine position. The details of catheter sizes and locations, the methods of sampling, the calibration of the densitometers, and the recording and preliminary reduction of data have been described.¹ A transfer function for the arterial segment lying between the femoral artery and the dorsalis pedis artery was obtained by considering the concentration-time curve recorded at the femoral artery as the input to a linear system and that recorded at the dorsalis pedis artery as the output.

MATHEMATICAL APPROACH TO THE USE OF THE CONVOLUTION INTEGRAL

The approach used in this study is essentially that of Stephenson:² the arterial system is considered subject to the types of analysis applicable to linear filters with lumped characteristics. It is assumed that the transfer function has its domain along only the time axis. This implies the secondary assumptions that each sampling site acts as a point and that the concentration at that point represents the amount of indicator per volume of fluid passing that point (that is, the concentration is volume-averaged)³, 4 or is the mean flow concentration.⁵ The transfer function of a linear system is a unique expression, $h(t)$, describing the gain and distortion of any signal passing through the system. $h(t)$ is the response of the network to a unit impulse as input. Given $h(t)$ and any input, $f(t)$, the output or system response, $g(t)$, has a unique description:

$$g(t) = \int_0^t h(t - \lambda) \bullet f(\lambda) d\lambda \tag{1}$$

or

$$g = f * h = h * f \tag{1a}$$

in which λ is a dummy variable of integration and $*$ is an abbreviation for the convolution. Equation 1 is the convolution integral, limited to systems which do not respond unless there is an input and in which $f(t) = 0$ for $t \leq 0$. The present experimental situation is represented in figure 1. Points 1, 2, and 3 represent the injection site and the sampling sites in the femoral artery and dorsalis pedis artery, respectively. Points 4 and 5 represent the densitometers whose outputs are the recorded concentration-time curves, $C_i(t)$ and $C_o(t)$, respectively. L_1 ; the vascular system between the injection site and the femoral sampling site, has a transfer function, $h_1(t)$, which is the response to a unit impulse, $\delta(t)$. Similarly, L_2 , the arterial segment between the two sampling sites, has a unit impulse response, $h_2(t)$. It is the purpose of these experiments to determine $h_2(t)$ under various circumstances. This cannot be done directly because a unit impulse cannot be introduced into the femoral artery (point 2) nor can the concentration, $g(t)$, at the dorsalis pedis artery (point 3) be obtained directly. The form of the injection cannot be characterized with current methods; therefore, the input function, $e(t)$, is unknown and the impulse response, $h_1(t)$, of system L_1 cannot be determined. $f(t)$ and $g(t)$ cannot be recorded directly but are distorted by the sampling systems, L_{S1} and L_{S2} .

The recorded curves are the arterial curves distorted by the sampling systems:

$$C_i(t) = f(t) * S_1(t) \tag{2}$$

and

$$C_o(t) = g(t) * S_2(t) \quad (3)$$

in which $S_1(t)$ and $S_2(t)$ are the sampling-system responses to a unit impulse. In these experiments the sampling systems have been designed to have nearly identical responses to a step change of dye concentration at the input¹ and, therefore, their time-domain transfer functions, $S_1(t)$ and $S_2(t)$, are very nearly identical:

$$S_1(t) = S_2(t) = S(t). \quad (4)$$

This simplifies the analysis considerably because then $C_o(t) = g(t) * S(t)$. Substituting for $g(t)$ by using equation 1a,

$$C_o(t) = h_2(t) * f(t) * S(t) \quad (5)$$

and then from equation 2,

$$C_o(t) = h_2(t) * C_i(t) \quad (6)$$

or more properly:

$$C_o(t) = \int_{-\infty}^{+t} h_2(\lambda) C_i(t - \lambda) d\lambda. \quad (7)$$

In the experimental situation the injection of indicator at time zero resulted in the concentrations C_1 and C_o , and therefore the lower limit of integration may be changed to ignore the zero concentrations preceding the injection:

$$C_o(t) = \int_0^t h_2(\lambda) C_i(t - \lambda) d\lambda. \quad (8)$$

The experimental determination of $h_2(t)$, hence-forth called simply $h_2(t)$, depends on the veracity of equation 8, which depends on $S_1(t)$ and $S_2(t)$ being equal and on the assumption of mathematical linearity. A consistent difference between $S_1(t)$ and $S_2(t)$ will result in a systematic error in the transfer function, but it was thought that the 0.25-second difference in the mean transit times of $S_1(t)$ and $S_2(t)$ present in this study was sufficiently small relative to an average mean transit time of 9 seconds for the transfer functions of these experiments that it could be ignored.

The determination of $h_2(t)$, is entirely dependent on the applicability of the superposition theorem. The requirements are that the system be linear and stationary.^{5, 6} (1) Stationarity means constant flow. (2) The indicator must travel in exactly the same fashion as the substance which it is considered to label. (In this experiment, plasma protein or perhaps simply plasma is labelled by indocyanine green but erythrocytes are not.) (3) There must be no loss or gain of indicator or its carrier during passage through the system between the femoral and dorsalis pedis arteries. (4) The sampling of the bloodstream for indicator concentration should be not only from all of the cross section of the vessel at the tip of the sampling system but also from each portion of this cross section in proportion to the flow across it (flow-averaged sample).⁵ (5) The system must also be linear such that, when

$$f_1(t) \rightarrow g_1(t)$$

and

$$f_2(t) \rightarrow g_2(t)$$

then

$$a_1 \bullet f_1(t - t_1) + a_2 \bullet f_2(t - t_2) \rightarrow a_1 \bullet g_1(t - t_1) + a_2 \bullet g_2(t - t_2).$$

Experimentally, t_1 or t_2 cannot be zero and therefore a test of linearity using the latter equation is dependent on the persistence of steady flow over a period of at least a few minutes.

While it is obvious that none of these conditions can be completely fulfilled, the deviations from ideal are not so great as to vitiate the practical application of superposition theory.⁷

COMPUTATION OF THE CONVOLUTION INTEGRAL

Digital computation of integrals of continuous functions is done by means of numerical approximations. The accuracy of a numerical integration is increased by decreasing the size of the intervals chosen. For these experiments, the interval, Δt , was 0.25 second which was 1/35 to 1/100 of the passage time of the primary curves. The functions $f(t)$, $h(t)$, and $g(t)$ are considered as sequences f_i , h_i , and g_i where i is an integer subscript valued 1 to n . f_i is the amplitude of a pseudo-impulse and substitutes for the area of $f(t)$ during a period, Δt , whose midpoint is t_i .

$$f_i = \int_{t_i - \Delta t/2}^{t_i + \Delta t/2} f(t) dt = \bar{f}(t_i) \bullet \Delta t.$$

The convolution integral (equation 1) was calculated in the recursive form:

$$\begin{aligned} g_1 &= f_1 h_1 \\ g_2 &= f_2 h_1 + f_1 h_2 \\ g_3 &= f_3 h_1 + f_2 h_2 + f_1 h_3 \end{aligned}$$

$$g_i = \sum_{j=1}^{i-1} f_j h_{i-j} + f_i h_1. \quad (9)$$

This Euler integration was found to be as accurate for these experiments as a Simpson's rule or a Runge-Kutta integration and was very much faster.

ESTIMATION OF THE TRANSFER FUNCTION

The transfer function appropriate to each pair of recorded curves, $C_i(t)$ and $C_o(t)$, was determined in terms of a suitably defined lagged normal density curve¹ whose equation is:

$$h(t) = \int_0^t \frac{1}{\sigma \sqrt{2\pi}} \cdot e^{-1/2 \left(\frac{\lambda - t_0}{\sigma} \right)^2} \cdot \frac{1}{\tau} e^{-\frac{(t-\lambda)}{\tau}} \cdot d\lambda, \quad (10)$$

in which t_c is the median of a normal density curve of standard deviation, σ , and τ is the time constant of a superimposed exponential (first order) lag. This model, which is the same one as that used by Nicholes and co-workers,⁸ was generated using a Runge-Kutta method. Values of $h(t)$ for $t < 0$ were ignored and, in practice, values were less than 0.5% of the peak value until $t > 0.5 (\tau + t_c)$. The curve was arbitrarily truncated on its downslope following the peak when values were less than 1% of the peak. The first, second, and third moments of $h(t)$ are, respectively, $\tau + t_c$, $\sigma^2 + \tau^2$, and $2\tau^3$.

It should be emphasized that this model is used to provide a concise numerical description of the transfer function. It is not unique, for several other models could be used, and there is no direct means of interpreting its parameters in physical terms, such as a velocity profile or other blood-flow characteristics. It is simply a stochastic, descriptive model which has been chosen on the basis of its mathematical similarity to equations for turbulent diffusion and the random walk and because, empirically, it does provide a sufficiently accurate description of the time-domain transfer function.

A trial transfer function, $h(t)$, was generated by using arbitrary values for σ , τ , and t_c and had values at intervals of 0.25 second. A trial output curve, $C'_o(t)$, was computed by the convolution of $C_i(t)$ and $h(t)$, by equation 9; $C'_o(t)$ was compared with $C_o(t)$ by determining the coefficient of variation. If the coefficient of variation was higher than a prescribed value, usually 0.005, then $h(t)$ was changed by adjusting the parameters of the lagged normal density curve, the convolution was repeated, and the new $C'_o(t)$ was compared with $C_o(t)$. This process was repeated either until the coefficient was less than the prescribed value or until 10 trials were completed, at which point the best result was printed out and plotted. The adjustment of the parameters was made automatically by the computer: if $C'_o(t)$ was too steep on the upslope, σ was increased; if $C'_o(t)$ was too steep on the downslope, τ was increased; if the peak was too early, t_c was increased. Interaction between the effects of these adjustments was taken into account (for example, an increase in τ also decreases the upslope and delays the peak) but there still tended to be a small oscillation about the best solution. This was seen when the prescribed goal for the coefficient of variation was set at an impossibly low value such as 0.002.

Results

USE OF THE LAGGED NORMAL DENSITY CURVE AS THE TRANSFER FUNCTION

The transfer function was determined in terms of a lagged normal density curve for 29 pairs of curves recorded after injection of indicator into the superior vena cava and for 28 pairs after injection into the aorta. Typical results are shown in figure 2. In each panel the computed downstream curve, $C'_o(t)$, represented by the + signs, is superimposed on the continuous line representing the dye curve recorded at the dorsalis pedis artery, $C_o(t)$. The parameters of the transfer function are listed in each panel. The coefficients of variation between $C'_o(t)$ and $C_o(t)$ were significantly ($P < 0.001$) less for pairs of curves recorded after injection of dye into the superior vena cava (mean coefficient of variation = 0.0053, $SEM = 0.0004$) than for those recorded after aortic injection (0.0094 ± 0.0008). The average for the 57 transfer functions was 0.0070 ± 0.0005 with a range from 0.002 to 0.020. In only four instances was the coefficient of variation greater than 0.011.

Under conditions of stationarity of flow, the transfer function of the segment during the period of recirculation should be the same as that for the dye passing the sampling sites for the first

time. The better-than-average result in the left upper panel of figure 2 shows this most clearly. Following aortic injection, the recirculation peaks were smaller because smaller amounts of dye were injected and because a larger proportion of the indicator goes into the vasculature of the lower part of the body, from which recirculation is much slower.⁹ Adjustment of the parameters of the transfer function was made in accordance with comparisons of the primary portions of curves $C_o(t)$ and $C'_o(t)$. As a result the later parts of the curves, representing recirculated indicator, did not match as well. This may be due to variability in the physiologic state (change of flow or distribution of flow) or perhaps variation in sensitivity or drift in base line of the densitometers during the recording.

The ratios of areas of the femoral curves to those at the dorsalis pedis artery averaged 0.96 ($SEM = 0.011$). The areas should be identical and the variation is an expression of the experimental error. Differences could be due to lack of stationarity, instrumental errors, or, least likely, to a difference in the error due to time-averaged sampling instead of volume-averaged sampling at the two sites.¹⁰ No significant change in sensitivity of the densitometers to known concentrations of dye in blood from the subjects was apparent on tests done periodically during each experiment. Lack of representative mixing was probably a minor factor because the variation in area was slightly greater following injections into the aorta. The systematic difference was due primarily to the error in extrapolation of the femoral curves (see fig. 5 of reference 1).

Lack of stationarity is a probable source of much of the variation noted in this study. Positive evidence of a change in flow is seen in figure 3. These data were recorded while the subject's physiologic status was apparently undisturbed and unchanging (no changes in heart rate, blood pressure, or respiratory rate). A sudden injection of dye was made into the thoracic aorta, and the upper pair of curves was recorded. The transfer function had the shape represented by the open circles in the left upper panel. The computed output curve, $C'_o(t)$, is superimposed on the recorded curve, $C_o(t)$, in the right upper panel (coefficient of variation = 0.006). Fifty seconds after the first injection, two injections of dye were made three seconds apart into the aorta, and the curves shown in the lower panels were recorded. As above, the transfer function, $h(t)$ (labelled "dispersion process"), and a theoretical output curve, $C'_o(t)$, were computed, and $C'_o(t)$ was compared with $C_o(t)$ in the lower right panel. The coefficient of variation was 0.010. Lack of stationarity is shown by the difference in mean transit time: $\tau + t_c$ equalled 14.5 seconds initially (upper panel) but was 13.5 seconds, less than a minute later (lower panel). If the change in flow occurred in the few seconds between these recordings, then both transfer functions may be valid. If a gradual change was occurring, then the error in each will be small. If the change occurred during the recording of one of the primary peaks the error would be quite significant. Differences of 0.5 to 1.0 second in \bar{t} were found fairly frequently even when the determinations were made at intervals as short as 50 seconds. This reflects presumably a continual variation in total blood flow in the leg or of distribution of flow in the leg vessels.

TEST OF THE MATHEMATICAL LINEARITY OF THE ARTERIAL SEGMENT

The data of figure 4 were obtained in a manner similar to those in figure 3, except that adenosine triphosphate was being infused into the right common iliac artery at a rate of 1.0 mg/min, producing a marked decrease in mean transit time and in dispersion. The mean transit time between sampling sites was the same (3.1 sec) after a single injection as it was, less than a minute later, after a pair of injections 4 sec apart. If this is taken as evidence for stationarity, then the curves may be used to test whether the transfer function is the same for input curves of widely differing form. The transfer function for the curves of the upper panel is described by a lagged normal density curve having $\sigma = 0.20$ sec, $\tau = 0.26$ sec, and $t_c = 2.8$ sec. That for the doubly peaked curves of the lower panels had $\sigma = 0.19$ sec, $\tau = 0.31$ sec, and $t_c = 2.75$ sec. The coefficients of variation were 0.007 and 0.011. The conclusion is that, when stationarity

is present, linearity was demonstrated by showing that the transfer function was independent of the shape of the recorded concentration-time curves. During infusion of adenosine triphosphate, stationarity was usually observed and five pairs of computed transfer functions obtained in the above manner were similarly independent of the form of the dye dilution curves. During the control state there were no consecutive pairs of transfer functions obtained at precisely constant flow or mean transit time and therefore linearity could not be tested.

RELATIONSHIPS BETWEEN PARAMETERS OF THE TRANSFER FUNCTION

The transfer function was determined only in terms of the parametric model, the lagged normal density curve. Figure 5 (left panel) shows that the square root of the variance, $(\sigma^2 + \tau^2)^{1/2}$, is linearly proportional to the mean transit time, $\tau + t_c$. That the shape was rather variable is shown by the relationships of σ and τ to $\tau + t_c$ (fig. 5, middle and right panels). The least-squares regression lines, calculated on the basis that error exists in values of ordinates and abscissas, have approximately the same slopes as observed¹ for the same relationships for the model fitted to the recorded dye curves. The large variation is a reflection of the fact that the shape of the transfer function is a caricature of the difference in the shapes of $C_i(t)$ and $C_o(t)$. The parameters σ and τ were unrelated ($\tau = 0.06$).

The theoretical values for \bar{t} and $\pi_2^{1/2}$ (the square root of the variance) were used in figure 5. The actual calculated moments gave slightly smaller values because the curve ordinates were computed at finite intervals (0.25 sec) and $h(t)$ was terminated when its value on the downslope was less than 1.5% of the peak value. As calculated, $\tau + t_o = 0.23 + 1.008 \bar{t}$ with a standard deviation of 0.033 and a correlation coefficient, r , of 0.999; similarly, $(\sigma^2 + \tau^2)^{1/2} = -0.08 + 1.13\pi_2^{1/2}$ ($sd = 0.051$, $r = 0.998$). These relationships should fall on the line of identity; such errors are more obvious with the higher moments.

The regression lines for the appearance time, t_a and $\bar{t} - t_a$ versus \bar{t} for $h(t)$ show relationships (fig. 6) similar to those obtained for the recorded curves. These lines might be expected to pass through the origin because there should be no influence from dispersion at the injection site or upstream from the arterial segment under study. That they do not, suggests that there may be some dependence of shape on the mean transit time. $\bar{t} - t_a$ is proportionately larger when \bar{t} is smaller, suggesting that $h(t)$ is more symmetric when \bar{t} is small. The same tendency is shown in the relationship between $\bar{t} - t_a$ and $\pi_2^{1/2}$ (fig. 6, right panel) and in the interrelationships between σ , τ , $\bar{t} - t_a$, and $\pi_2^{1/2}$. For example, $\sigma = -0.07 + 2.24(\bar{t} - t_a)$ ($sd = 0.24$, $r = 0.73$); this is very close to the ratio, $\sigma/(\bar{t} - t_a) = 0.26$. Thus, the relationship $\sigma = 0.45 + 0.19 \pi_2^{1/2}$ ($sd = 0.33$, $r = 0.38$) must and does show a positive ordinate intercept, while values of τ were relatively small when \bar{t} and $\pi_2^{1/2}$ were small (fig. 5, right panel). $\tau = 0.51 + 1.23 \pi_2^{1/2}$ ($sd = 0.30$, $r = 0.94$) and $\tau = -0.92 + 0.82(\bar{t} - t_a)$ ($sd = 0.60$, $r = 0.72$).

Table 1 reflects the same tendency. The variations in σ/\bar{t} and in τ/\bar{t} were so great that no significant differences due to injection site were seen. The average ratios are similar to those obtained previously¹ for recorded dye curves but are smaller following aortic injections, $\pi_2^{1/2}/\bar{t}$ was significantly ($P < 0.02$) less with aortic injections. Similarly, the average $(\bar{t} - t_a)/\bar{t}$ was smaller and t_a/\bar{t} was larger for aortic injections.

COMPARISON OF TRANSFER FUNCTION WITH RECORDED CURVES

The shape and variance of the transfer function may be compared with the recorded curves. Figure 7 illustrates the relationships of the first and second moments of the transfer function to those of the recorded curves. They should follow the line of identity. The systematic deviation of the second moments from the relationship, $\pi_{2h} = \pi_{2DP} - \pi_{2F}$ (the subscripts *DP* and *F* indicate the downstream [dorsalis pedis] and upstream [femoral] curves, respectively), is due in part to integration error and to truncation error in the calculation. The scatter observed

may be expected in a comparison of an error-containing parameter, $(\sigma^2 + \tau^2)^{1/2}$, with the relatively small difference between two large and some-what erroneous values, π_{2DP} and π_{2F} .

Discussion

LAGGED NORMAL DENSITY CURVE AS A MODEL

The purpose of these experiments was to compute a transfer function which was independent of the influences of dispersion at the site of injection and of distortion by the sampling system. Since these factors unavoidably affect the recorded concentration-time curve, use of this curve as the transfer function, as Zierler¹¹ advocated, serves only as a rough approximation.

In order to ascertain the transfer function without using transforms, $h(t)$ may be assumed and adjusted by some trial and error process until a suitable $h(t)$ is found. Tedious as this is, such a method has certain advantages because it avoids the division of the frequency-domain transform of the recorded output curve by that of the input curve. Such a division is akin to differentiation, and when the data are not smooth but have random or systematic variation superimposed on the ideal $C_o(t)$ and $C_i(t)$, the solution tends to have wide fluctuations and may oscillate. Stephenson² predicted this, and it has also been observed by Paynter¹² and by Parrish and co-workers.¹³ The use of the iterative computation of the output function in the time domain (equation 9) is akin to integration or the use of linear filters and, because $h(t)$ is smooth, it results in $C'_o(t)$ being smoother than $C_i(t)$ or $C_o(t)$.

A model is used because it provides convenience in defining and adjusting $h(t)$. The lagged normal density curve is thought to be easier to adjust than other models whose forms are not visualized so readily from the parameters. It is a better model for the transfer function than it is for recorded curves. For the 57 determinations, the average coefficient of variation between $C_o(t)$ and $C'_o(t)$ was 0.007, which appears to be almost an order of magnitude better than the 0.056 found when comparing the model to the recorded curves.¹ The improvement is not so great as these numbers would imply because the calculation comparing $C'_o(t)$ to $C_o(t)$ uses the data points beginning at the appearance time of $C_o(t)$ and ending at the last data point during the recirculation; this produces a relative increase in the denominator and reduces the coefficient of variation.

Various probability models could very likely be used as a transfer function in the manner demonstrated here. This has not been attempted in this study, but the cascaded delay lines used by Parrish and co-workers¹³ form transfer functions very similar to a normal density curve. The response of a single delay line to a step input is a symmetric sigmoid curve which is remarkably similar to a normal distribution curve.* Theirs is a complex model but, since each delay line may be roughly approximated by a normal density curve, a cascade of n such units in series may be described by:

$$h(t) = \sum_{i=1}^{i=n} \frac{A_i}{\sigma \sqrt{2\pi i}} \cdot e^{-1/2 \left(\frac{t - i\Delta t}{\sigma \sqrt{i}} \right)^2} \tag{11}$$

in which i is the position of the delay line in the series, A_i is the coefficient for each delay line

and $\sum_{i=1}^{i=n} A_i = 1.0$, Δt is the mean delay time of one unit, and σ is the square root of the variance

*For graphic illustrations, see "Time domain synthesis based on a passive tardigrade module." *In Lightning Empiricist*: 11 (3) July, 1963. Boston, G. A. Philbrick Researches, Inc.

of $h(t)$ for one unit. Thus, the system is describable by the $n + 2$ parameters, C_i , Δt , and σ . If the nonzero coefficients are all equal, then $h(t)$ will be symmetric. Skewing to the right was produced by having higher coefficient settings for the longer delay lines than for the shorter. If only one coefficient were used, then the model would be virtually identical to the lagged normal density curve. The virtuosity of the Parrish model could be greatly extended and the number of parameters reduced by the inclusion of exponential lags and, even in its present state, could encompass the situation in which there are parallel systems with different mean transit times. This, of course, can also be done with the lagged normal density curve by using the sum of two curves as a transfer function. Recirculation to the heart by separate systemic pathways can be described only in such terms.^{7,8,14,15}

MATHEMATICAL LINEARITY OF THE VASCULAR SYSTEM

The most formidable requirement for linearity is stationarity.⁵ Zierler¹⁶ has said, "If phasic, not necessarily regular, alterations in distribution of transit times fluctuate rapidly about some central value, and if the periods of the phases are brief compared to the time required for evolution of the sudden-injection indicator concentration-time curve, then the violation of stationarity may not be important." The same condition reduces the error induced by time-averaged sampling of the flowing blood. It is then not surprising that the coefficients of variation were smaller for the broad curves following injections into the superior vena cava, because the passage time of the aortic curves may be as short as 5 to 7 sec.

Variation in vasomotor activity and in peripheral flow, as observed by Burton¹⁷ and Allwood and Burry,¹⁸ is a more significant source of error. Figure 3 illustrates that this does not necessarily prevent the calculation of transfer functions, but their validity must be doubted because it is not known when the change of flow occurred. In certain instances the flow must have increased during the period the indicator was passing the distal sampling site because $C_o(t)$ was narrower than $C_i(t)$ and the calculation of a transfer function was ridiculous. For such reasons, similarity of area is a good criterion for selection of pairs of curves from which to determine the transfer function.

Nicholes and co-workers⁸ described a test for linearity, with which they obtained a satisfactory result. Injections of 0.5, 1.0, and 2.0 times the usual amount of dye were made into the superior vena cava, and the blood was sampled from the pulmonary artery. The resulting concentration-time curves had the same shape, and their areas were in proportion to the dye dose. This test confirms both the laws of conservation of material and the basis for the use of dye techniques to measure flow, but it is not a critical test of linearity because the shape of the primary portion of the dye curve is so ubiquitous. Transfer functions for indicator recirculating to the pulmonary artery were calculated from the primary curve (C_i) and the "first recirculation" curve (C_o) but were inconstant, which probably reflects the lack of stationarity of flow in the peripheral vascular system.

The test shown in figure 4 is a good test of linearity over a specific vascular segment but, since the two injections (lower panels) were 4 sec apart and the transfer function was short, the two peaks remained separate throughout the segment. The shape of the curves changed very little from those in the upper panels and therefore the criticism must be made that there is not a great difference in the form of $C_i(t)$ in the upper and lower panels. The assumption of linearity has been justified by experiments in which transfer functions were obtained simultaneously for three segments of the aorta in dogs.⁷

INTERRELATIONSHIPS BETWEEN PARAMETERS OF THE TRANSFER FUNCTION

The curves recorded at the two sampling sites have been shown¹ to be basically similar in shape. The transfer function should therefore also have the same shape. The output curve, C

$'_o(t)$, computed by means of the convolution integral, must always have a degree of skewness or kurtosis intermediate between those of the input curve $C_i(t)$ and the transfer function $h(t)$, and it will be more spread out than either. For example, the lagged normal density curve is the convolution of a normal density curve and a single exponential curve; it is neither as skewed as the exponential nor as symmetric as the Gaussian curve. Therefore, when $C_i(t)$ and $C_o(t)$ differ in shape, the transfer function, $h(t)$, must be more skewed than $C_o(t)$ if $C_o(t)$ is more skewed than $C_i(t)$. Or, if σ/\bar{t} of the model fitting $C_o(t)$ is greater than is σ/\bar{t} of the model fitting $C_i(t)$, then σ/\bar{t} of $h(t)$ must be greater than τ/\bar{t} of $C_o(t)$ and τ/\bar{t} of $h(t)$ must be less than τ/\bar{t} of $C_o(t)$. The statement regarding τ follows from the fact that the variance of $C_i(t)$ plus the variance of $h(t)$ should equal the variance of $C_o(t)$. In other words,

$$\pi_{2_f} + \pi_{2_h} = \pi_{2_g} \tag{12}$$

or

$$(\sigma_f^2 + \tau_f^2) + (\sigma_h^2 + \tau_h^2) = (\sigma_g^2 + \tau_g^2) \tag{13}$$

coupled with the empirical observation that $\pi_2^{1/2} = 0.18 \bar{t}$, which holds approximately for both the recorded curves and the transfer function (fig. 5 and table 1). This phenomenon of the transfer function exaggerating the differences between $C_i(t)$ and $C_o(t)$ is similar to the exaggeration of irregularities produced by differentiating a function. This is the main reason for the poor correlation between σ or τ and \bar{t} (fig. 5), and it results in the apparently random relationship between σ and τ .

The relationships of t_a and $(\bar{t} - t_a)$ to \bar{t} (fig. 6) show much less scatter than do those of σ or τ to \bar{t} . The difference between the average transit time and the shortest transit time is closely related to the variance of the transfer function (right panel) and a quick and approximate estimate of the variance could be obtained by the equation $\pi_2^{1/2} = 0.55 (\bar{t} - t_a)$. This value is a rough average for the relationships of figure 5.

The observation that $\pi_2^{1/2}/\bar{t}$ and $(\bar{t} - t_a)/\bar{t}$ had smaller average values (table 1) following aortic injection might suggest that the dispersion in the arterial system of the leg is influenced by the site of injection. Such a thought is contrary to physiologic and mathematical expectations, and the deviation is probably due to a small systematic experimental error.

RELATIONSHIPS OF PARAMETERS OF THE TRANSFER FUNCTION TO PARAMETERS OF THE RECORDED CURVES

In table 2 are listed the average values of the slopes of the relationships of various parameters to the mean transit times of the recorded curves¹ (left column) and the slopes obtained for the parameters of the transfer function (right column). These slopes and the ratios of the transfer function parameters to \bar{t} (next to last column, table 1) should be influenced only by dispersion within the vascular segment between the sampling sites. The similarity in the values indicates that a rather good prediction of the transfer function could be made from the parameters of the recorded curves.

The relationship between the transfer function mean transit time and the difference in mean transit times between the curves recorded from the densitometers is obviously a necessary one and should fall on the line of identity if the sampling systems are identical (fig. 7, left panel). Some variation is expected because the three mean transit times necessary to plot each point are calculated independently. Greater error is found in the estimates of variance principally because of errors in the tails of the curves, and the variation from the line of identity (equation

12) is larger (fig. 7, right panel). Computation error is greater for the higher moments and produces a systematic underestimation.

SPATIAL AND TEMPORAL DISTRIBUTION OF INDICATOR PARTICLES

Because of the proportionality of spread to mean transit time and because of the small influence of flow on this relationship, certain statements can be made about $C(x, t)$, the distribution of the indicator particles with respect to distance x along the system. In general, if any two of the following are known, then the third may be calculated: (1) $C(x_1, t)$ at a point in the system x_1 ; (2) $C(x_1, t)$ the spatial distribution of concentration with respect to distance at a particular time t_1 ; (3) the rate of increase of spread of $C(x)$ with time. This is somewhat oversimplified since details such as cross-sectional versus flow sampling must be considered also.

One way of looking at these phenomena is to consider a system in which there is constant proportionality of distribution of flow. Such a system might have turbulent or laminar flow but the simplest example is a system (fig. 8) consisting of a number of parallel pathways, each having piston flow and each carrying a constant proportion of the total flow. (Piston flow defines the velocity to be the same at all points in a cross section of the tube.) Indicator injected at point A in such a system will be dispersed, if the pathways have varied mean transit times, at a given total flow rate, Q . It is obvious that, under these conditions, when an impulse input is made at A, the spatial distribution, $C(x)$, will be the same around B no matter what the flow rate is. The temporal distribution at the point B, $C(t)$, is a function of the spatial distribution and of the flow rate. Let the curve at the lower left corner of the figure represent $h_1(t)$ when the flow is stationary at Q_1 ml/sec. The amount of indicator and the time for it to travel from A to B through pathway D is given by the rectangle at time, t_{D1} .

In a geometrically stable system the flow rate and mean transit time are related reciprocally:

$$V = Q_1 \bar{t}_1 = Q_2 \bar{t}_2 \tag{14}$$

in which V is the Stewart-Hamilton or the mean transit time volume of the system and need not be defined anatomically. Equation 14 is applicable to the portion of the circulatory network (including branches) in which there is constant proportionality of distribution of flow. As a result, the transfer functions, $h(t)$, at different flow rates are related by:

$$h_2(t) = \frac{\bar{t}_1}{\bar{t}_2} \cdot h_1\left(\frac{\bar{t}_1}{\bar{t}_2} \cdot t\right) = \frac{Q_2}{Q_1} \cdot h_1\left(\frac{Q_2}{Q_1} \cdot t\right). \tag{15}$$

The scale factor, $\bar{t}_1/\bar{t}_2 = Q_2/Q_1$, is necessary to keep the transfer function at unit area. When the concentration-time curves are related in the same fashion:

$$C_2(t) = C_1\left(\frac{\bar{t}_1}{\bar{t}_2} \cdot t\right) = C_1\left(\frac{Q_2}{Q_1} \cdot t\right) \tag{16}$$

then the peak heights, C_{1p} and C_{2p} , are the same and the areas are inversely related to the flow, Q . Similarly, $C(t_{D2}) = C(t_{D1})$ and $C(t_{E2}) = C(t_{E1})$ while $t_{D2} = Q_1 t_{D1} / Q_2$, and $t_{E2} = Q_1 t_{E1} / Q_2$. This may be viewed merely as normalization of the time scale to t/\bar{t} .

The model illustrated in figure 8 is a generalized streamline flow model. The parameters of the spread of $C(t)$, viz., $\pi_2^{1/2}$, $\bar{t} - t_a$, σ , τ , and any others, are in constant proportion to \bar{t} . These relationships will apply to any constant-volume streamline flow model over any range of flows

so long as the requirement for constant proportionality of flow in each stream is fulfilled. They, and also equations 14, 15, and 16, apply equally well to any turbulent or disturbed flow system of constant volume in which the mean velocity profile is unchanged by flow changes. Because the systemic pressure was constant in each subject despite large changes in femoral artery flow, it is not surprising that the arterial volume was quite constant. It is unlikely that the highly distensible venous system would have so little change in volume over such a range of flows.

The restriction of geometric stability and constant proportionality of distribution may be relaxed to some extent in an open-ended system such as that between the femoral artery and the dorsalis pedis artery. Stationarity need only be maintained in the main arterial stream between these two points. Thus, the distribution of flow to each primary branch must be constant, but in secondary branches the flow need not be clearly defined. The boundaries of the volume, V , may be changed at will within the second and higher order branches of the system.

It is important to realize that streamline flow is not necessarily implied by the observations of this study. The generalized flow model has been discussed because it is simple and because streaming flow is probable in the vascular system, even though true laminar flow is not, because of the presence of erythrocytes. Any type of turbulent flow whose spatial dispersion is related linearly or nonlinearly to the distance traveled and not to the flow will give similar results. The six-fold range of mean transit times of $h(t)$'s indicates a similar range of flows, the highest of which would result in Reynolds numbers of about 2,000 in the femoral artery if the flow were not pulsatile. It seems unlikely that laminar flow could persist at such flows even if the artery were a uniform cylinder. The similarity of the relationship of spread to mean transit time at low flows to that at high flows, where turbulence is almost certainly present, suggests that flow is usually turbulent. Turbulence may be expected at relatively low flows of nonhomogeneous fluids driven by a pulsatile head of pressure through elastic, branched, tapering, curved tubes. On the other hand, "complete" turbulence resulting in constant concentration over the cross section of the artery and in longitudinal dispersion of indicator seems little more probable than Newtonian laminar flow. Most likely, a compromise model embodying longitudinal and lateral dispersion superimposed on some rather blunt velocity profile will turn out to be the most realistic.

ROLE OF CIRCULATORY DISPERSION IN STUDIES ON DIFFUSIBLE INDICATORS

After injection of a bolus containing diffusible and nondiffusible indicators, simultaneous concentration-time curves for the several substances may be obtained by sampling from the venous outflow of an organ. Such data can be used to estimate the volume of distribution of each indicator and rates of transfer of diffusible indicators from the bloodstream into the tissue.¹⁹⁻²¹ Combination of this knowledge with information on the mode of transport within various vascular segments should produce relatively complete descriptions of the movement of a substance from one tissue to another, and complex models of the whole body or of single organ systems could be formed without some of the simplifying assumptions made by Jacquez and co-workers.²²⁻²³

Acknowledgments

Dr. Earl H. Wood not only made this work possible but also aided in the initiation and execution of the experiments and in the revision of the manuscript. The author also thanks Dr. Homer R. Warner, Department of Biophysics and Bio-engineering, Latter Day Saints Hospital, University of Utah, for his role in starting the project. Mrs. Jean Frank and her co-workers assisted in the preparation of the illustrations. Dr. K. K. Nicholes helped in developing the initial programs.

Supported in part by Research Grants HE-04664 and FR-00007 from the National Institutes of Health, U. S. Public Health Service.

References

1. Bassingthwaighte JB, Ackerman FH, Wood EH. Applications of the lagged normal density curve as a model for arterial dilution curves. *Circulation Res* 1966;18:398. [PubMed: 4952948]
2. Stephenson JL. Theory of the measurement of blood flow by the dilution of an indicator. *Bull. Math. Biophys* 1948;10:117. [PubMed: 18884373]
3. Visscher MB, Johnson JA. The Fick principle: Analysis of potential errors in its conventional application. *J. Appl. Physiol* 1953;5:635. [PubMed: 13044747]
4. Stow RW. Systematic errors in flow determinations by the Fick method. *Minn. Med* 1954;37:30. [PubMed: 13119623]
5. González-Fernández JM. Theory of the measurement of the dispersion of an indicator in indicator-dilution studies. *Circulation Res* 1962;10:409. [PubMed: 13900229]
6. Meier P, Zierler KL. On the theory of the indicator-dilution method for the measurement of blood flow and volume. *J. Appl. Physiol* 1954;6:731. [PubMed: 13174454]
7. Bassingthwaighte JB, Ackerman FH, Essex HE. Mathematical linearity of the dog's arterial system. *Federation Proc* 1965;24:335.
8. Nicholes KK, Warner HR, Wood EH. A study of dispersion of an indicator in the circulation. *Ann. N. Y. Acad. Sci* 1964;115:721. [PubMed: 14214047]
9. Nicholes KK, Warner HR, Toronto AF, Bassingthwaighte JB. Effect of exercise on the distribution of transit times of an indicator through various routes in the systemic circulation. *Federation Proc* 1963;22:523. (abstr.).
10. Bassingthwaighte JB, Edwards AWT, Wood EH. Areas of dye-dilution curves sampled simultaneously from central and peripheral sites. *J. Appl. Physiol* 1962;17:91. [PubMed: 13865655]
11. Zierler, KL. Circulation times and the theory of indicator-dilution methods for determining blood flow and volume. In: Hamilton, WF.; Dow, P., editors. *Handbook of Physiology*. Vol. vol. 1. Washington, D. C.: 1962. p. 585-615. *Circulation, Am. Phys. Soc.*
12. Paynter HM. Methods and results from M.I.T. studies in unsteady flow. *Boston Soc. Civil Engr. J* 1952;39:120.
13. Parrish, Daniel; Hayden, DT.; Garrett, Wayne; Huff, RL. Analog computer analysis of flow characteristics and volume of the pulmonary vascular bed. *Circulation Res* 1959;7:746. [PubMed: 14430598]
14. Sheppard, CW. An electromathematical theory of circulatory mixing transients. *Proceedings of the First National Biophysics Conference; Yale University Press; 1959. p. 476-492.*
15. Sato, T.; Takahashi, K.; Dohi, Y. The IV World Congress of Cardiology. Mexico City: 1962 Sep. Critical study of the Hamilton-Stewart principle for hemodynamic analysis; p. 312-313.
16. Zierler KL. Theoretical basis of indicator-dilution methods for measuring flow and volume. *Circulation Res* 1962;10:393.
17. Burton AC. The range and variability of the blood flow in the human fingers and the vasomotor regulation of body temperature. *Am. J. Physiol* 1939;127:437.
18. Allwood MJ, Burry HS. The effect of local temperature on blood flow in the human foot. *J. Physiol* 1954;124:345. [PubMed: 13175136]
19. Chinard FP, Enns T, Nolan MF. Indicator-dilution studies with "diffusible" indicators. *Circulation Res* 1962;10:473. [PubMed: 13878999]
20. Goresky CA. A linear method for determining liver sinusoidal and extra-vascular volumes. *Am. J. Physiol* 1963;204:626. [PubMed: 13949263]
21. Zierler KL. Theory of use of indicators to measure blood flow and extracellular volume and calculation of transcapillary movement of tracers. *Circulation Res* 1963;12:464.
22. Jacquez JA, Bellman R, Kalaba R. Some mathematical aspects of chemotherapy. II. The distribution of a drug in the body. *Bull. Math. Biophys* 1960;22:309.
23. Bellman R, Jacquez JA, Kalaba R. Some mathematical aspects of chemotherapy. I. One-organ models. *Bull. Math. Biophys* 1960;22:181.

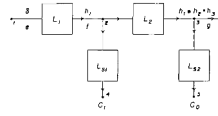
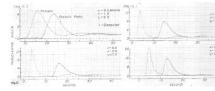


FIGURE 1.

Block diagram of the experimental situation. Point 1 (left) is the injection site, 2 is the tip of the femoral sampling system, 3 is the tip of the sampling system in the dorsalis pedis artery, and 4 and 5 are the recorded outputs of the densitometers of the femoral and dorsalis pedis sampling systems.

**FIGURE 2.**

Use of a lagged normal density curve as the transfer function relating pairs of time-concentration curves. The pair of curves (continuous lines) in each panel were recorded simultaneously from the femoral and dorsalis pedis arteries. Femoral curves were convoluted with lagged normal density curves whose parameters, σ , τ , and t_c are listed. Computed output curves (+ signs) closely approximate the recorded dorsalis pedis curves. Coefficients of variation between these computed and recorded output curves were 0.003, 0.007, 0.009, and 0.012. The average coefficient of variation for all the experiments was 0.007. Curves in the left upper panel, recorded after injection into the superior vena cava, illustrate one of the best results. Aortic injections were used to produce the other curves.

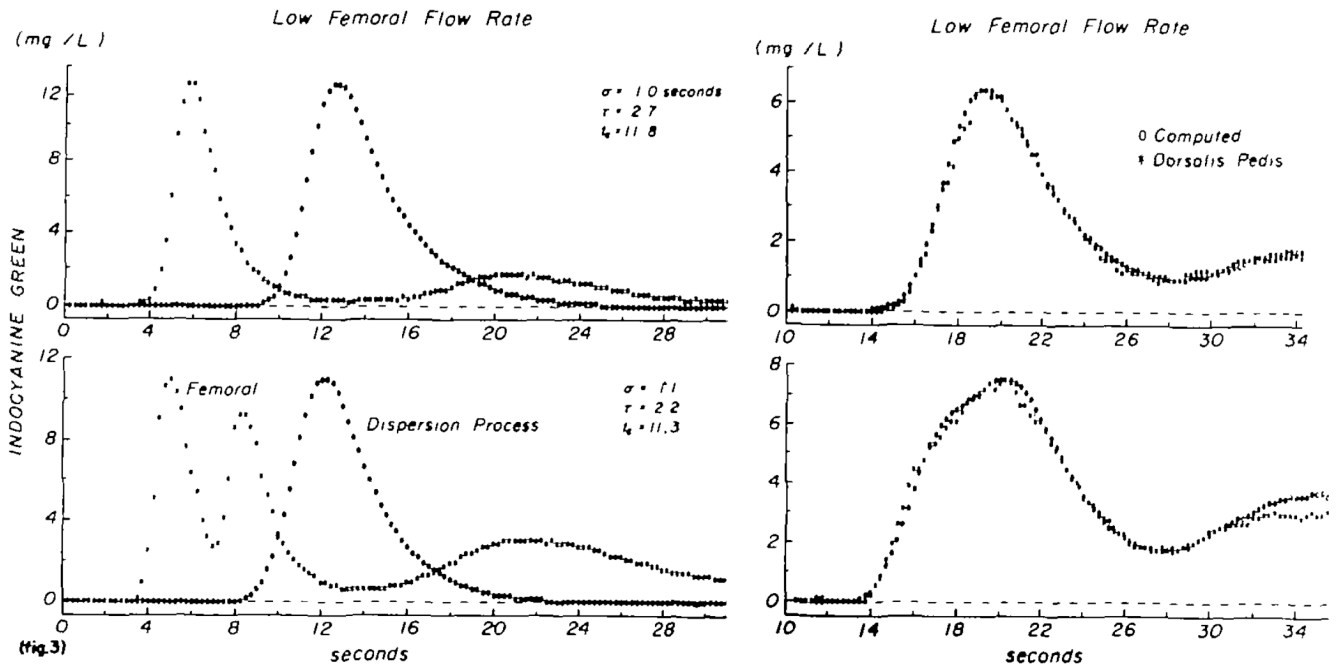


FIGURE 3.

Test of constancy of the transfer function at normal femoral flow rate. Left panels: curves recorded from the femoral artery (asterisks) and the calculated transfer function (zeros) whose parameters are listed and whose amplitude was 1. Right panels: curves recorded at the dorsalis pedis artery (asterisks) and the computed output curve (zeros). Upper panels: single injection into the thoracic aorta. Lower panels: two single injections 3 sec apart. Mean transit time ($\tau + t_c$) after the single injection was 14.5 sec and after the double injection, 13.5 sec. This inconstancy was typical and prohibits the use of these curves as a test of linearity.

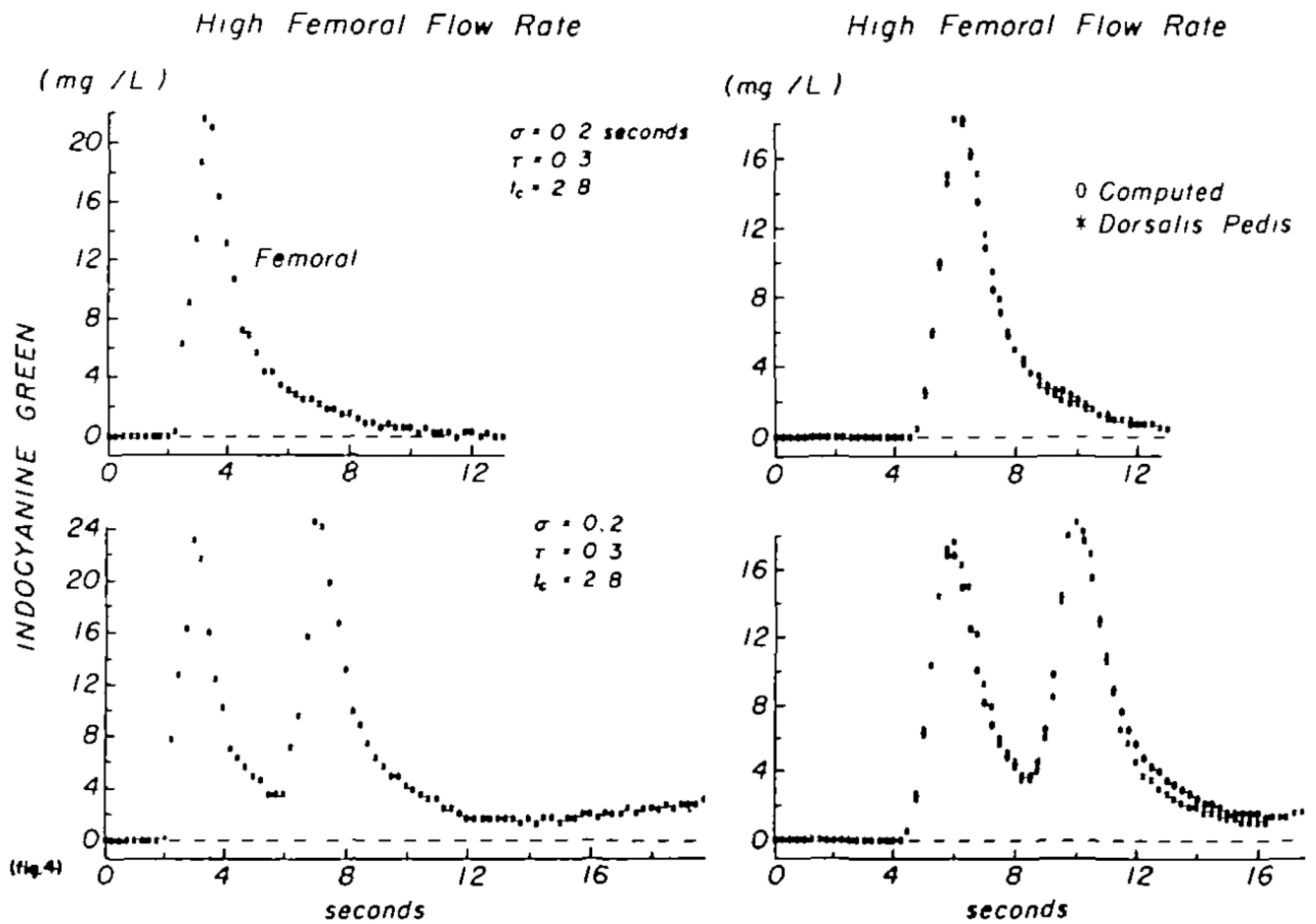
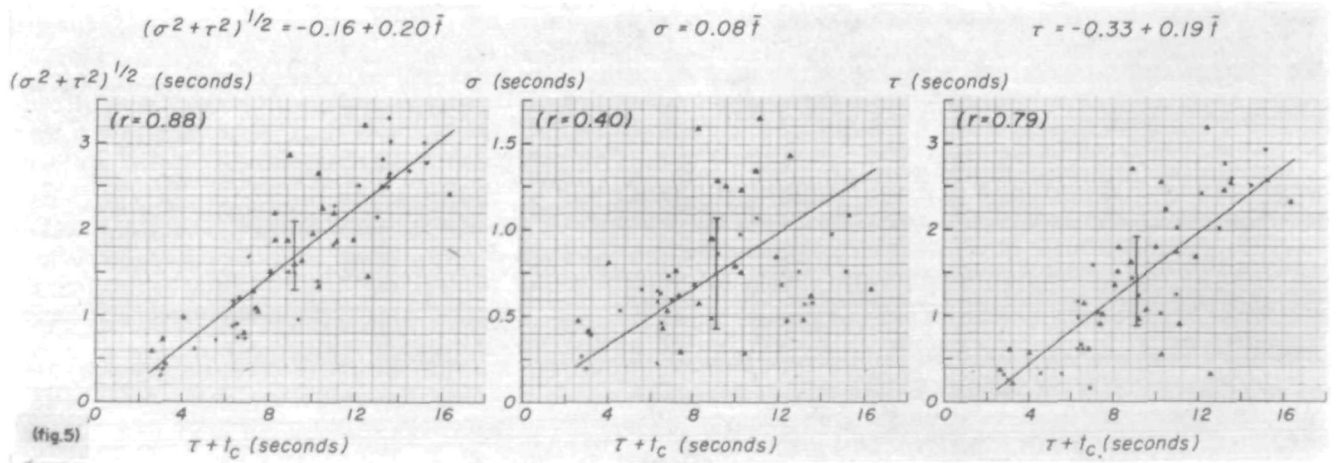


FIGURE 4. Test of the constancy of the transfer function at a high femoral flow rate (during infusion of adenosine triphosphate into the common iliac artery at a rate of 1.0 mg/min). The situation is similar to that of figure 3. Lower panels: two injections 4 sec apart. In this case the mean transit time remained constant at 3.1 sec and the transfer function was also the same despite the difference in form of the two curves, thereby suggesting that the arterial segment may be considered to behave as a linear system.

**FIGURE 5.**

Parameters of the model simulating the transfer function. Left panel dispersion, as estimated by the square root of the variance of the transfer function, $(\sigma^2 + \tau^2)^{1/2}$, is linearly related to the mean transit time, $\tau + t_c$ (which equals \bar{T}), in a manner similar to that seen for the recorded curves. Middle and right panels: σ and τ of the transfer function exhibit very scattered, approximately linear relationships to $\tau + t_c$. Triangles denote data recorded following injection into superior vena cava; +’s or x’-s denote injection into the aorta. Length of the vertical line at the average point is two standard deviations.

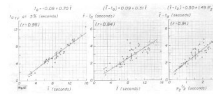


FIGURE 6.

Dispersion of the transfer function. The relationships of t_a and $(\bar{t} - t_a)$ to the mean transit time between the sampling sites are similar to those relating the corresponding parameters of the recorded curves, but the scatter is significantly greater. The positive Y-intercept in the relationship between $(\bar{t} - t_a)$ and $\pi_2^{1/2}$ suggests that the shape of the transfer function is slightly affected by the flow rate. Symbols as in figure 5; t_a is defined as the time at which $h(t)$ first exceeds 3% of its peak value.

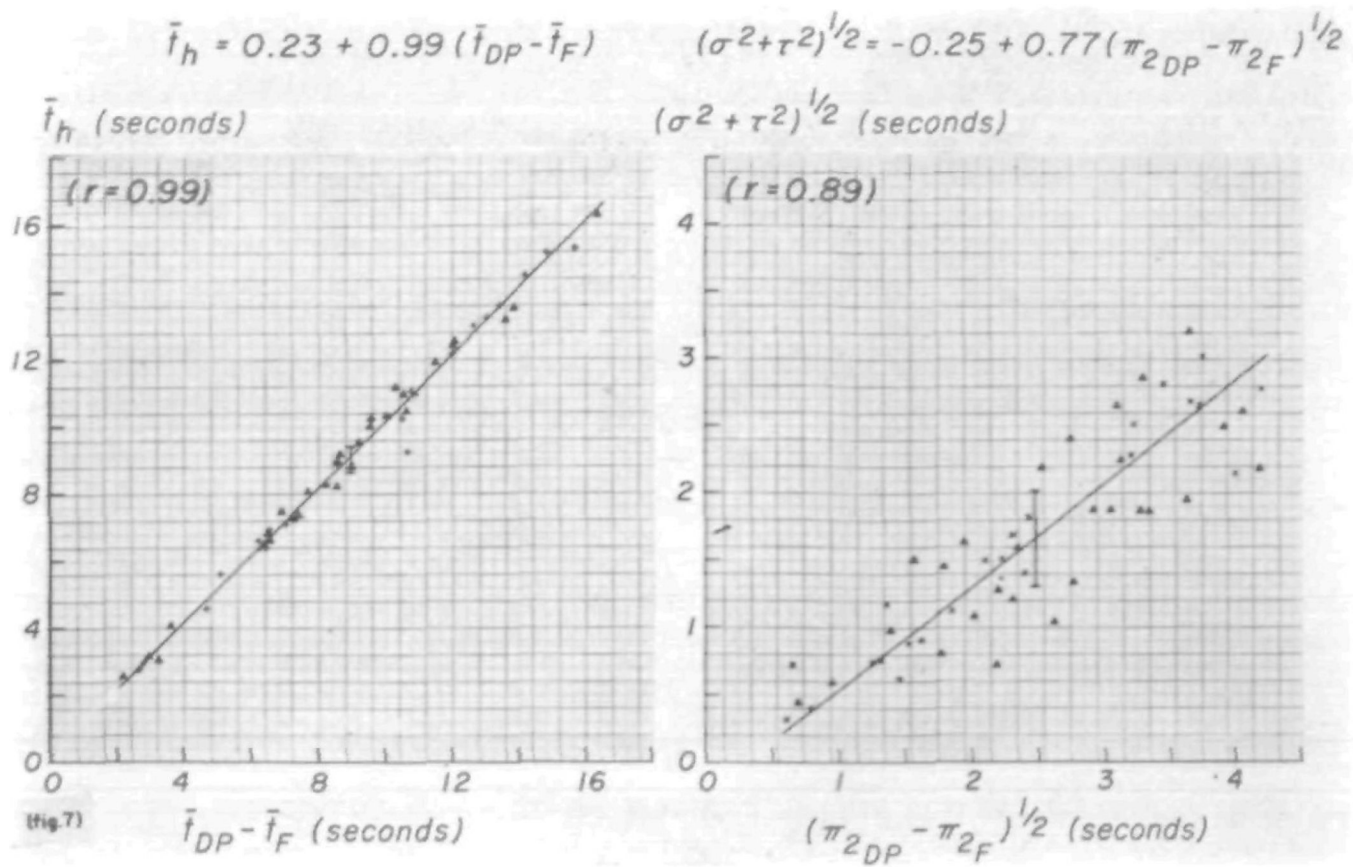
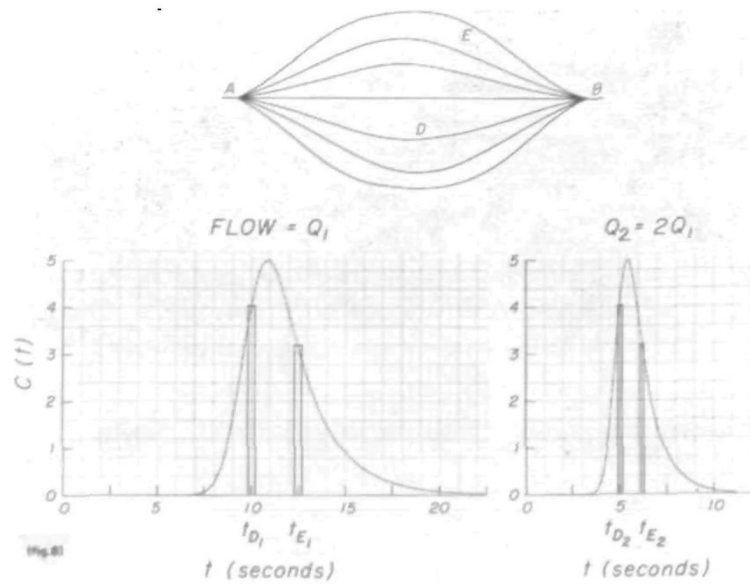


FIGURE 7. Relationships between moments of the transfer function and moments of the recorded curves. The systematic deviation of the relationship between the variances, the second moments, is partly due to error in computing π_2 .

**FIGURE 8.**

Diagrammatic representation of the effect of change of flow rate in a generalized flow system. When the rate is doubled, the dilution curve is halved in area and the transit time through any particular path, D or E, between A and B is also halved. In such a system the various measures of the breadth of concentration-time curves are linearly related to the mean transit time.

TABLE 1

Ratios of Parameters of the Transfer Function

Ratio	Injection site											
	Superior vena cava				Aorta				All curves			
	N	Mean ± SE	SD	N	Mean ± SE	SD	N	Mean ± SE	SD	N	Mean ± SE	SD
σ/\bar{t}	29	0.101 ± 0.009	0.050	28	0.080 ± .005	0.027	57	0.091 ± 0.005	0.040			
τ/\bar{t}	29	0.165 ± 0.012	0.068	28	0.146 ± 0.011	0.059	57	0.156 ± 0.008	0.063			
$\pi_2^{1/2}/\bar{t}^*$	29	0.191 ± 0.009	0.049	28	0.162 ± .006	0.033	57	0.177 ± 0.006	0.041			
$(\bar{t}-t_0)/\bar{t}^*$	28	0.386 ± 0.020	0.106	28	0.330 ± .009	0.046	56	0.358 ± 0.011	0.081			
t_d/\bar{t}^*	28	0.614 ± 0.020	0.106	28	0.670 ± .009	0.046	56	0.642 ± 0.011	0.081			

* Difference between injection sites is statistically significant ($P < 0.02$).

TABLE 2
 Comparison of Slopes Relating Parameters to Mean Transit Times for Recorded Curves and for Those of the Transfer Function

Slope of relationship with \bar{t}	Recorded curves*			Transfer function		
	N	Slope	SD [†]	N	Slope	SD [†]
σ	118	0.070	0.18	57	0.082	0.33
τ	116	0.149	0.43	57	0.16	0.54
$\pi_2^{1/2}$	118	0.181	0.48	57	0.182	0.36
$\bar{t}-t_h$	118	0.30	0.73	57	0.30	0.60
t_h	118	0.70	0.73	57	0.70	0.60

* Data from Bassingthwaighte and co-workers.¹

[†] SD = 1 standard deviation of regression line at the mean \bar{t} , which was 15.0 sec for the recorded curves and 9.1 sec for the transfer functions.